Behavior of existing piled raft foundation due to tunnel excavation

E. Sung, H. M. Shahin, M. Yamamoto, T. Nakai & M. Hinokio
Department of Civil Engineering, Nagoya Institute of Technology, Nagoya

ABSTRACT

Two dimensional model test and numerical analysis were carried out to investigate the behaviors of existing piled raft and group pile due to tunnel excavation. It is revealed from the model tests and the numerical analyses that the distribution of earth pressure and the profiles of ground settlement are different in case of existing load from the results of green field conditions, forming unsymmetrical shape. The ground deformation and the behavior of piled raft are influenced by the existing load. The behaviors of group pile are also influenced according to the location between tunnel and piles.

1. INTRODUCTION

As a lot of structure exist alongside the road where tunnel is usually excavated, the interaction of existing structure and tunneling should properly be considered during tunnel construction. This interaction could be thought in two cases. One is the influence of tunnel construction on existing piles, and the other is the influence of pile construction and loading on existing tunnels. Especially, the effect of tunneling to the pile foundation not yet fully understood, when there is pile foundation above the tunnel. Recently, several studies to this interaction problem have been published. Loganathan et al (2001) presented the methods for the lateral response of piles located close to tunnel construction. They explained the lateral and axial responses of piles caused by tunneling using a two- stage approach. First, free-field movements due to tunnel construction are estimated based on an analytical method, and then these estimated ground movements are imposed on the pile in simplified boundary value analyses to compute the pile responses. Jacobsz et al (2004) published the study about the behavior of single driven pile due to tunneling. They discussed about the changes of pile settlement, base load and shaft friction in dense sand using Centrifuge test. And they also presented the affected area for pile settlement due to tunneling. Shahin et al (2004) presented the numerical analysis and plane strain trap door test for tunnel earth pressure and ground settlement considering footing.

This paper reports 2D model test and numerical analysis to investigate the effects of tunneling near group pile and piled raft. Firstly, earth pressure and ground settlement are checked. Then, the change of load of the pile as well as the raft is presented with excavation step. Here, it is also investigated the change of pile load and shaft friction capacity by the initial overburden load. In this paper, every pile is located above the tunnel. All the model tests and numerical analyses were carried out assuming that the initial stress in the ground and piles is affected by the existing building load.

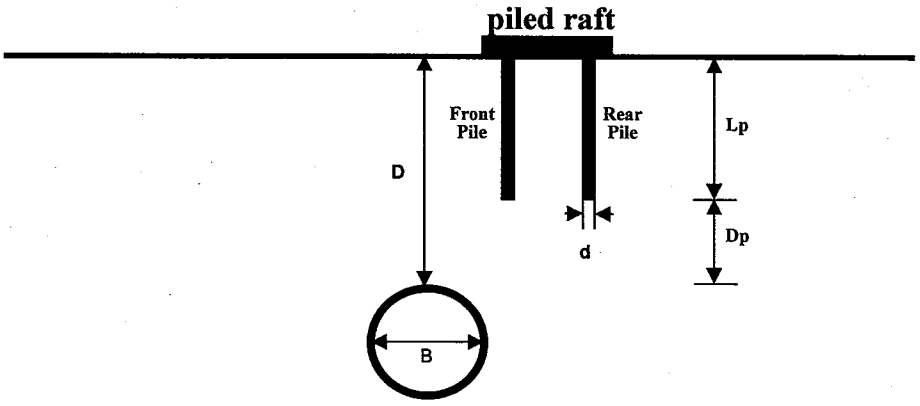

Fig. 1: Interaction of pile foundation and tunnel

2. DESCRIPTION OF MODEL TESTS

Figures 2 and 3 represent the trap door apparatuses for group pile and piled raft used in the model tests, respectively. The apparatus consists of 10 brass blocks (blocks A to J) of 8cm in width each, and set along the centerline of an iron table. Ground is made with mass of aluminum rods, having diameters of 1.6mm and 3.0mm mixed in a ratio of 3:2 in weight. The unit weight of the aluminum rod mass is 20.4 kN/m^3, and length is 50mm. After the installation of pile in the ground, tunnel excavation is started by downward movement of block F until 4mm.In the every excavation step, earth pressure is measured by 3 load cell blocks, each of which consists of 4 load cells. And, the surface settlement is measured by using a laser type displacement transducer. The references (Nakai et al., 1997 and Shahin et al., 2004) describe the details of the apparatus.

Piled raft (or cap) is made by aluminum plate, of 8cm in length and 2cm in thick. Pile is made by polyurethane, and the Young's modulus of this material is $80.9*10^3$ kN/m^2. In our research work, we call this type pile as flexible pile. The pile material is chosen assuming a similarity ratio of 1:100 between the model test and prototype. The thickness of the pile is 0.5cm and the length is varied according to the pattern of the test.

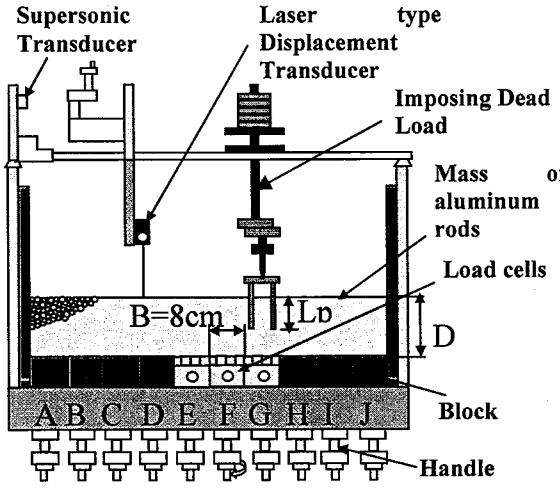

Fig. 2: Trap door apparatus for group pile

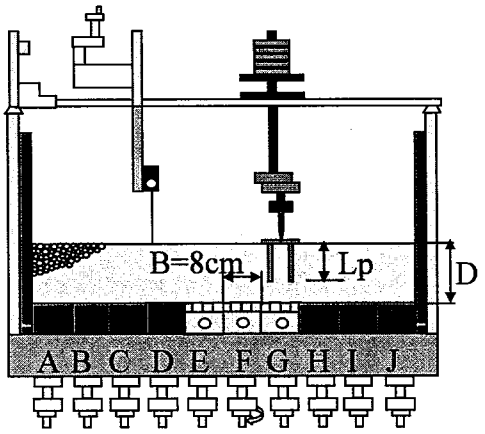

Fig. 3: Trap door apparatus for piled raft

The model tests and the numerical analyses are carried out for two types of deep foundation of the structure, one is for group pile and the other is for piled raft. For both deep foundations, three patterns of tests are performed which is shown in Table 1. In this research, the model tests are conducted for 2 kinds of soil covers, D/B equals 2.0, 3.0, and D_p/B equals 1.0, 2.0. Here, D is the depth of ground surface to the top of the tunnel, B is the width of trap door, and D_p is the vertical distance between the pile tip and the tunnel block. The same amount of the dead load (Q_v=3.2 N/cm) was used for comparison between group pile and piled raft in the model tests and numerical analyses.

Table 1. Model tests

Case	D/B	D_p/B
1	2.0	1.0
2	3.0	2.0
3	3.0	1.0

3. NUMERICAL ANALYSIS

Figure 4 shows the mesh used in the finite element analyses. Finite element analyses are conducted considering plane strain drain condition. Isoparametric quadrilateral elements are used in the mesh. Both vertical sides of mesh are free in the vertical direction, and the bottom face is fixed. To simulate the tunnel excavation, vertical displacement is applied until 4mm to the nodes which correspond to the tunnel block.

The constitutive law used in this numerical analysis is the subloading t_{ij} model (Nakai and Hinokio, 2004). The model parameters are represented in Table 2. Figure 5 shows the results of the biaxial tests for the mass of aluminum rods. From the results it is seen that the mass of aluminum rods has a property of the positive and negative dilatancy like dense sand. In the figure, the dotted line represents the numerical results for a confined pressure of 1/100 times about the confined pressure of the experiments. From figure 5, it is noticed that the subloading t_{ij} model can express the dependency of stiffness, strength and dilatancy on density and confining pressure. And, it can be understood that the subloading t_{ij} model can express softening behavior of the mass of aluminum rods very well. In the numerical analyses, the initial ground stress is calculated by the simulation of the self-weight consolidation. This simulation is made by imposing the pressure from very small confining pressure to the self weight ($\gamma = 20.4kN/m^3$) in the condition of one dimensional consolidation.

The elastoplastic joint element (Nakai, 1997) is used at the beneath of the raft and at the face of the piles. The friction angle (δ) of the joint element is 18° that was obtained by the laboratory test. In all numerical analyses, the elements of the pile and the raft (cap) were modeled as a linear elastic material with large stiffness.

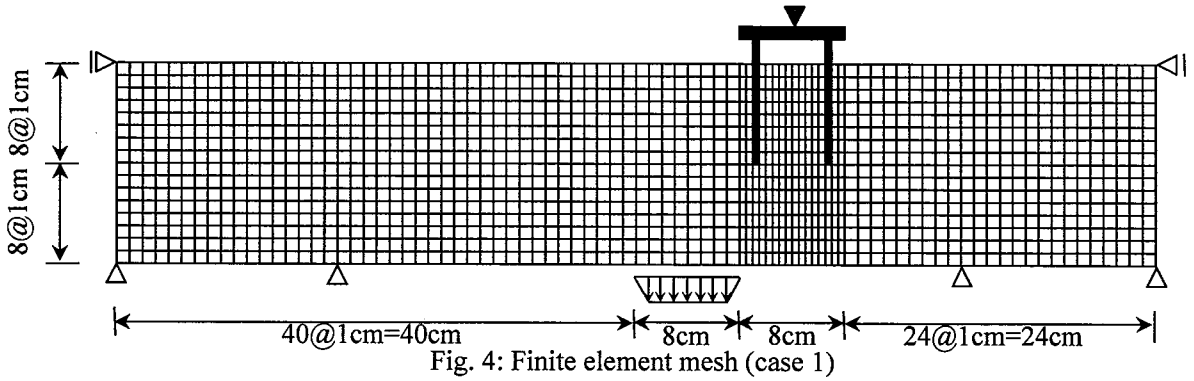

Fig. 4: Finite element mesh (case 1)

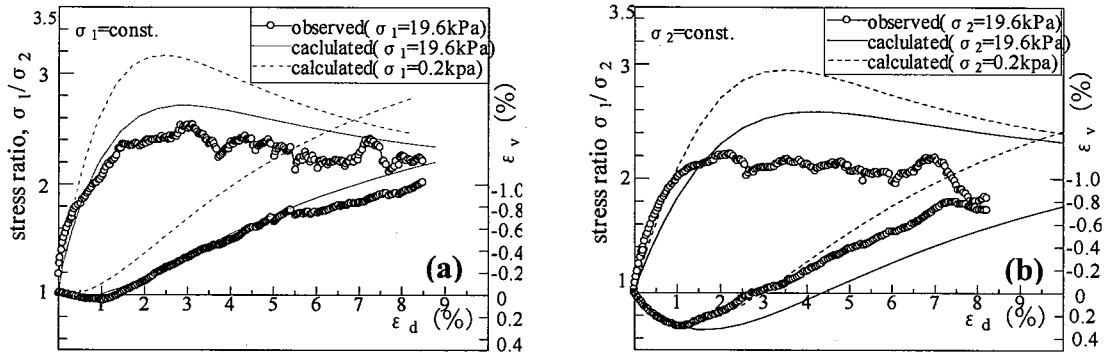

Fig. 5: Stress-strain-dilatancy relation of the mass of aluminum rods

Table 2. Parameters of soil materials

λ	κ	$N\,(e_{NC}\ at\ p=98kPa\ \&=0kPa)$	$R_{CS}=(\sigma_1/\sigma_3)_{CS(comp.)}$	β	ν_e	a
0.008	0.004	0.30	1.80	1.20	0.20	1300

4. RESULT AND DISCUSSION

4.1 Earth pressure and surface settlement

Figure 6 represents the earth pressure at the level of the lowering block of the group pile due to tunneling, where (a) is the results of the model test and (b) is the numerical analysis. Figures 7(a) and (b) also represent the distribution of earth pressure of the model tests and the numerical analyses at the level of the lowering block for the piled raft. The solid line without marks shows the result of the earth pressure for the green field. From these figures, it can be seen that the distribution of earth pressure for existing group pile or piled raft is different from that for the green field condition. Especially, at the place of the installed pile the vertical stress distribution is very different than that of the green field condition due to the initial stress condition. Figure 8 is the distribution of the deviatoric strain ($\varepsilon_1 - \varepsilon_3$) for all test patterns of the piled raft together with the green field conditions. It is seen in this figure that the shear band of the ground is developed during excavation for both piled raft and green field conditions. However, because of the disturbed initial stress, the development of the shear band is different between the left and the right side of the excavation block from the initial excavation step, which results the unsymmetrical distribution of earth pressure in case of the piled raft. The shear band is formed from the excavation block to the position of the front pile in case of D_p is equal to 8cm, which is seen in figures 8(a) and 8(c). In contrast, the shear band is extended from the right side of the excavation block to the position of the rear pile in case of D_p is equal to 16cm as seen in figure 8(b). From the initial step, the development of deviatoric strain in the right side of excavation block is faster than the left side. However, the direction of the deviatoric strain close to the surface is changed to the pile due to the high initial stress around the pile. These deformation patterns of ground would lead to change the behavior of the group pile and the piled raft.

Figures 9 and 10 represent the surface settlements for the model tests and numerical analyses both for the group pile and the piled raft. It is revealed in these figures that the settlement profiles for the existing group pile or piled raft are different from the green field condition. For both cases the maximum settlement occurs at the place of the existing structure. The maximum settlement is larger than the green field condition for this amount of applied load. It is also noticed that the inclination of the group pile or piled raft depends on the distance between the pile tip and the excavation

block (D_p). The closer the pile tip from the excavation block, the more inclination of the existing structure towards the excavation place is seen.

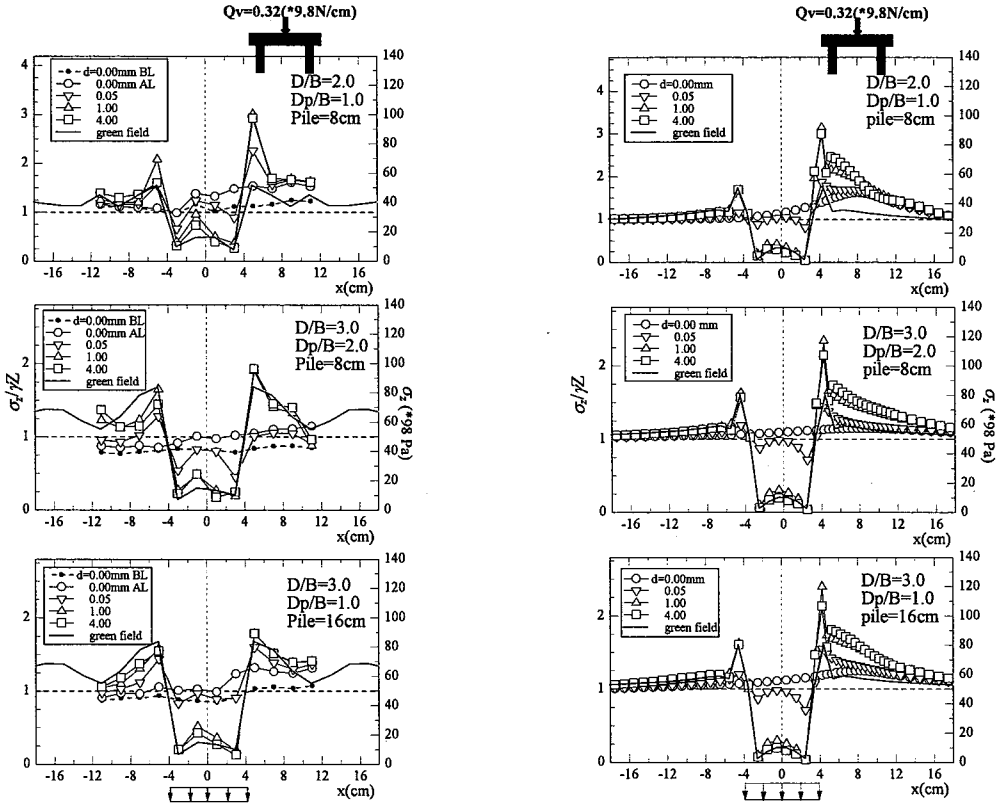

(a) results of experiments (b) results of analysis

Fig. 6: Distribution of earth pressure for the group pile

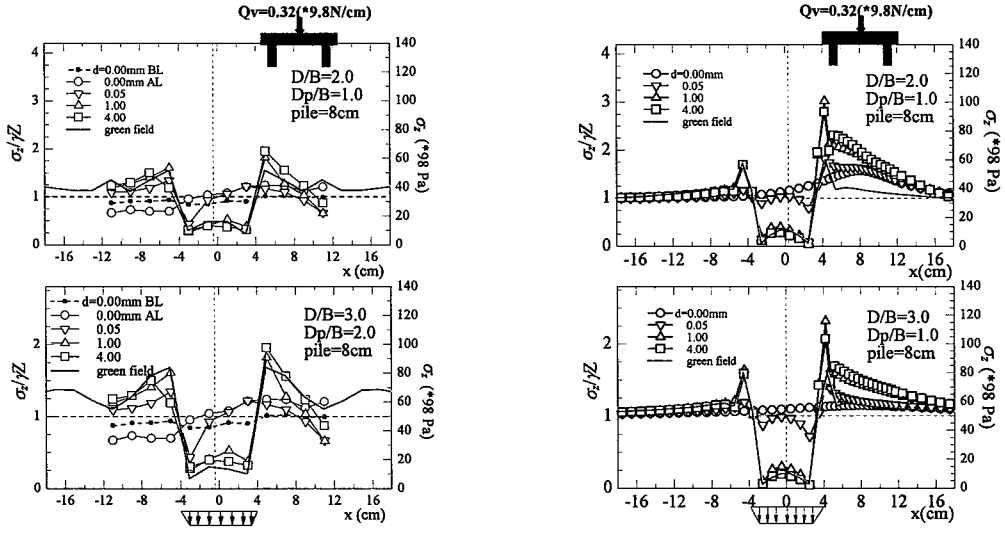

(a) results of experiments (b) results of analysis

Fig. 7: Distribution of earth pressure for the piled raft

Figures 11 and 12 show the deformation of the model ground and the computed displacement vectors for the group pile and piled raft for lowering block F, respectively. The deformation of model ground is obtained by superimposing two photos, the first one was taken after imposing dead load and before lowering the block, and the other was after lowering the block by 4mm. (Shahin et al. 2004). It is revealed in this figure that the deformation zone in case of D/B= 2.0, 3.0 and D_p/B =1.0 spreads towards the tip of the front pile from the top of the lowering block, which is different from the result observed for the green field. And, it can be seen from Figures 11 and 12 that the raft (or cap) is rotated to the direction of the excavation except D/B=3.0 and D_p/B =2.0. In case of D/B=3.0 and D_p/B =2.0, deformation spreads towards the head of the rear pile both for the piled raft and the group pile. So, the cap of the group pile and the raft of the piled raft are not rotated to the direction of the tunnel but in the opposite direction.

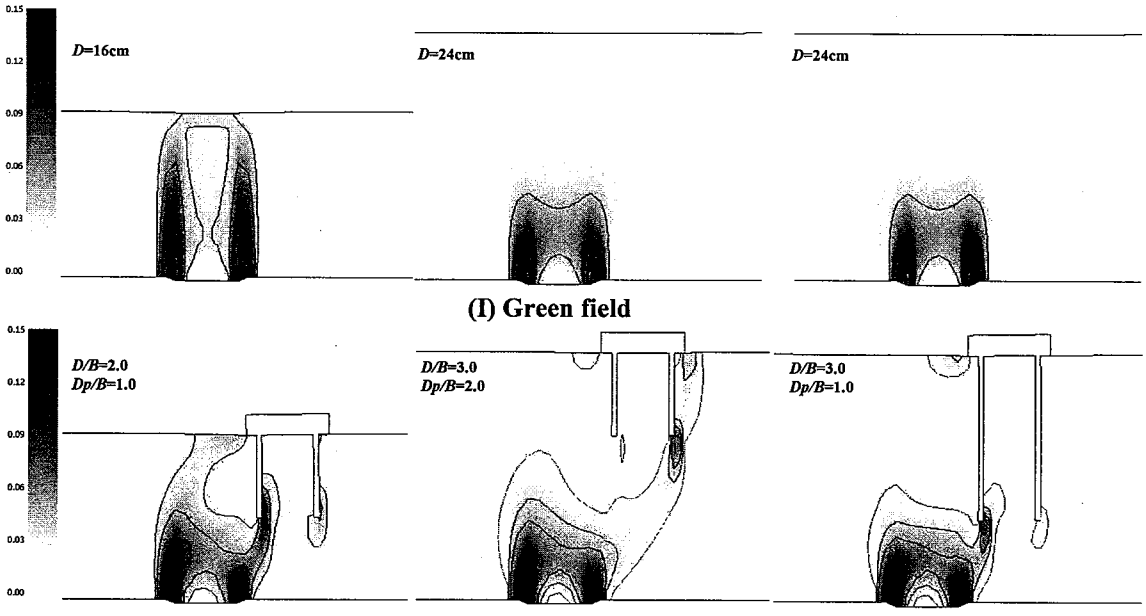

(a) case 1 (b) case 2 (c) case 3

Fig. 8: Distribution of deviatoric strain contour (after excavation)

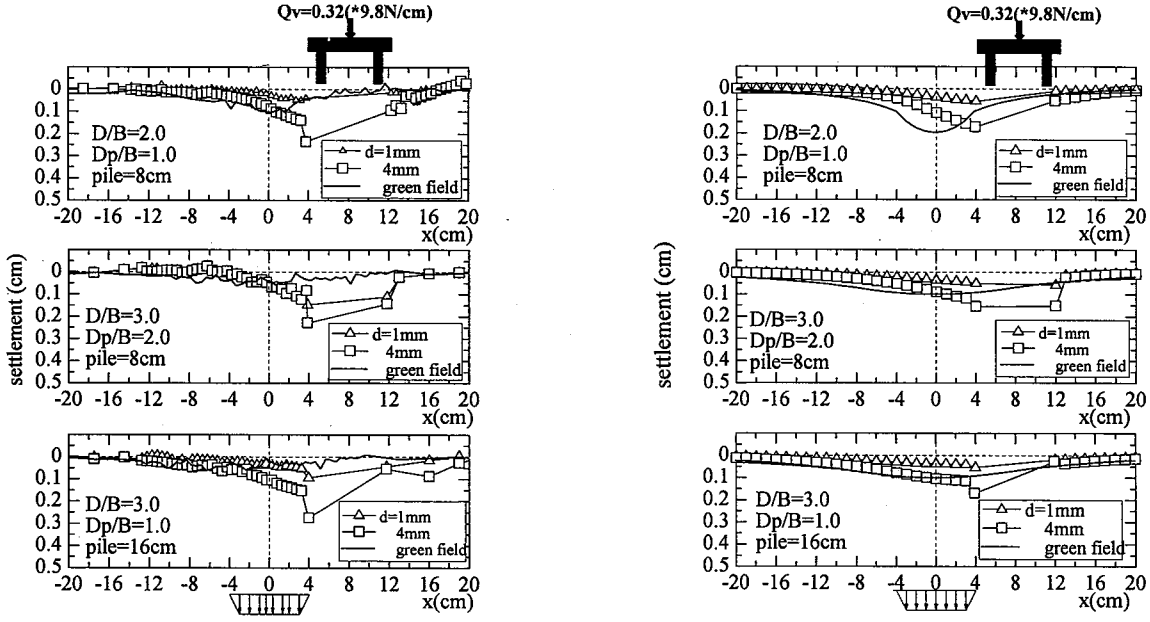

(a) results of experiments (b) results of analysis

Fig.9: Surface settlement for the group pile

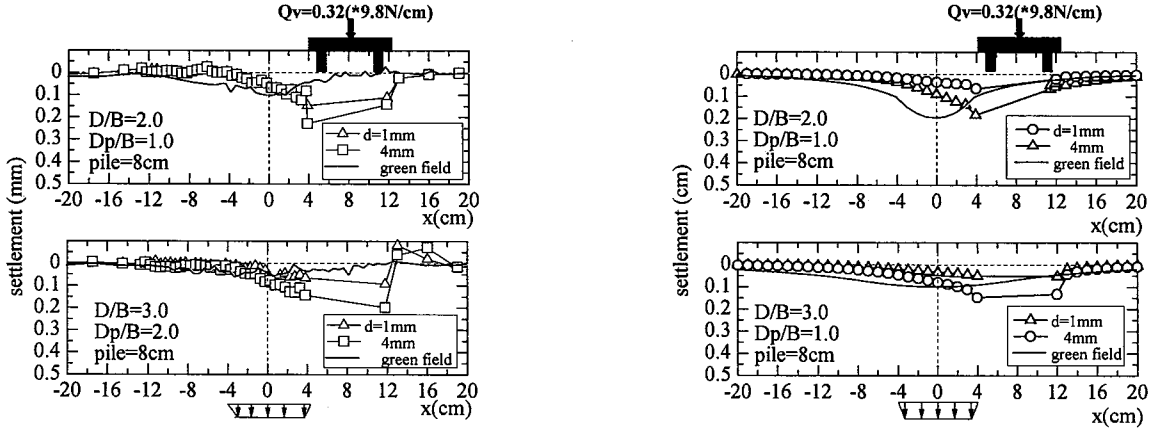

(a) results of experiments (b) results of analysis

Fig.10: Surface settlement for the piled raft

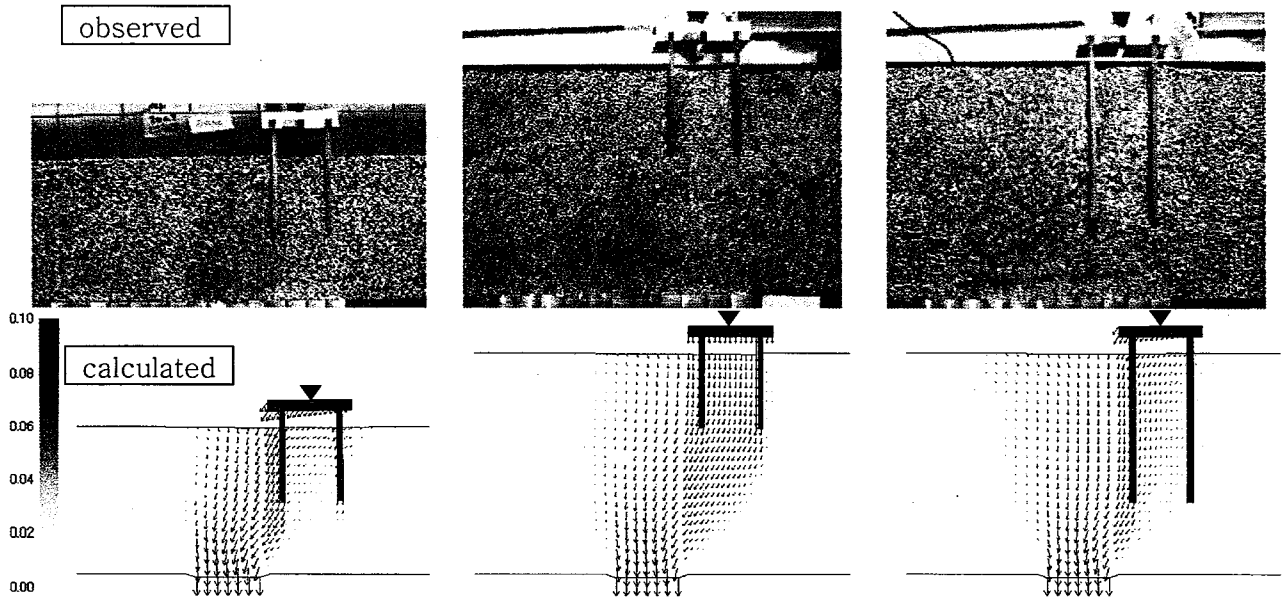

(a) case 1 (b) case 2 (c) case3

Fig. 11: Deformation zone of the model test and displacement vector of the group pile

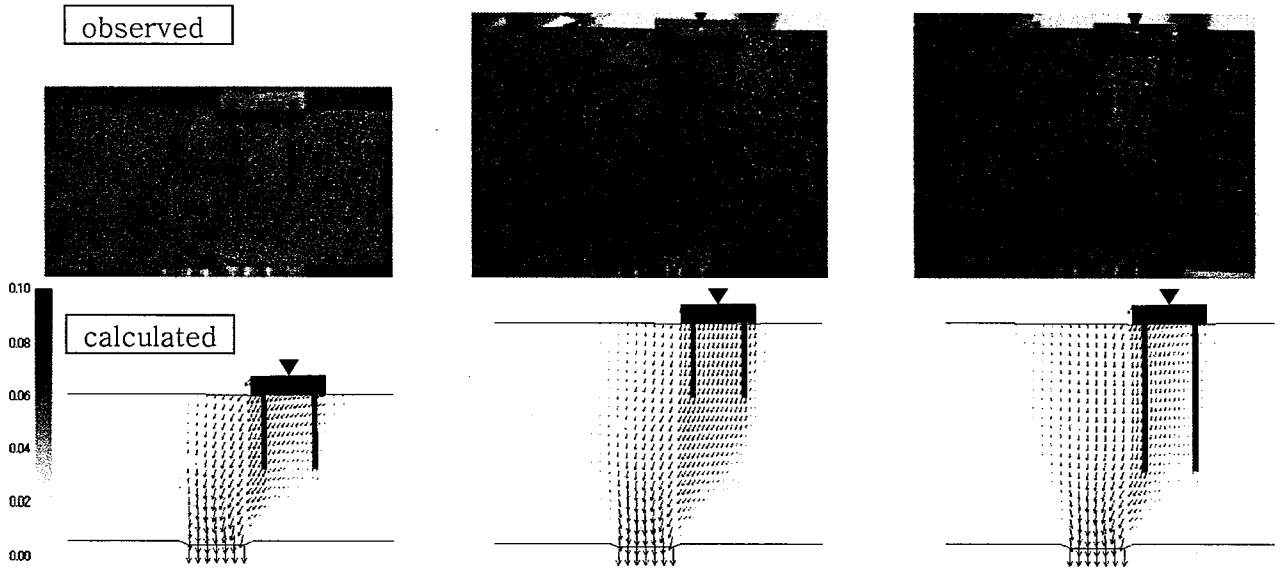

(a) case 1 (b) case 2 (c) case 3

Fig. 12: Deformation zone of the model test and displacement vectors for the piled raft

4.2 Piled raft behavior due to tunneling

Figure 13 represents the cpmputed distribution of the axial load for the piled raft at different stage of the tunnel excavation in case of D/B = 2.0 and 3.0. The figures are drawn with the same scale of the pile length. In Figures 13(a) and (b) the length of the pile is 8cm, and in Figure 13(c) the length of the pile is 16cm. Figure 13(a) represents the results of D/B = 2.0, and Figures 13(b) and (c) represent the results of D/B = 3.0. In all the cases, the vertical axial load of the pile changes; the vertical axial load of the front pile which is nearer to the excavation block decreases with the excavation of the tunnel due to the release of the tip bearing stress and the relative movement of the pile and the surrounding soils. On the other hand, the vertical axial load of the rear pile which is far from the excavation block increases with the excavation of the tunnel. The change of the vertical axial load of the pile is seen significantly in case of D_p/B=1.0. For D_p/B=2.0 (Figure 13(b)), the change of the vertical axial load of the pile is less significant. From this point, it can be said that the change of the vertical axial load of the pile depends on the distance between the tip of the pile and the excavation block. Figure 14 shows the distribution of the contact normal load beneath the raft at different stage of the tunnel excavation. The contact normal load beneath the raft increases with the excavation of the tunnel. As the vertical load of the front pile (nearer to the excavation block) decreases, the vertical load of the raft increases more.

In case 1, where the pile length is 8cm, a significant increase of the vertical load of the raft is seen for the large reduction of the load at the front pile.

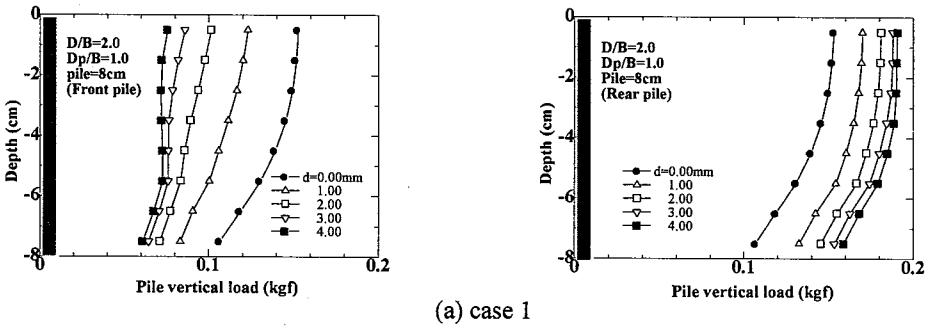

(a) case 1

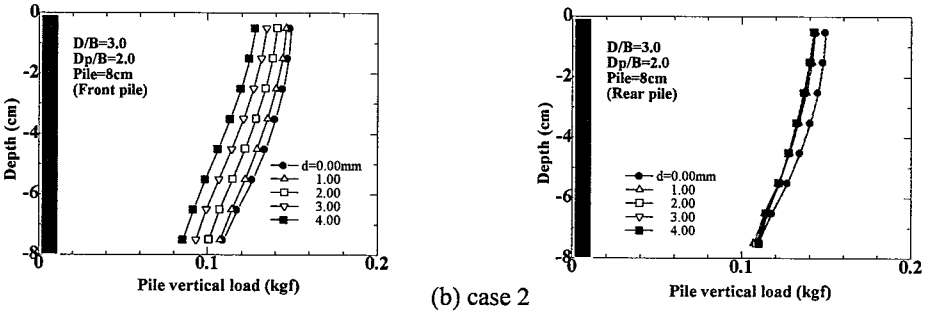

(b) case 2

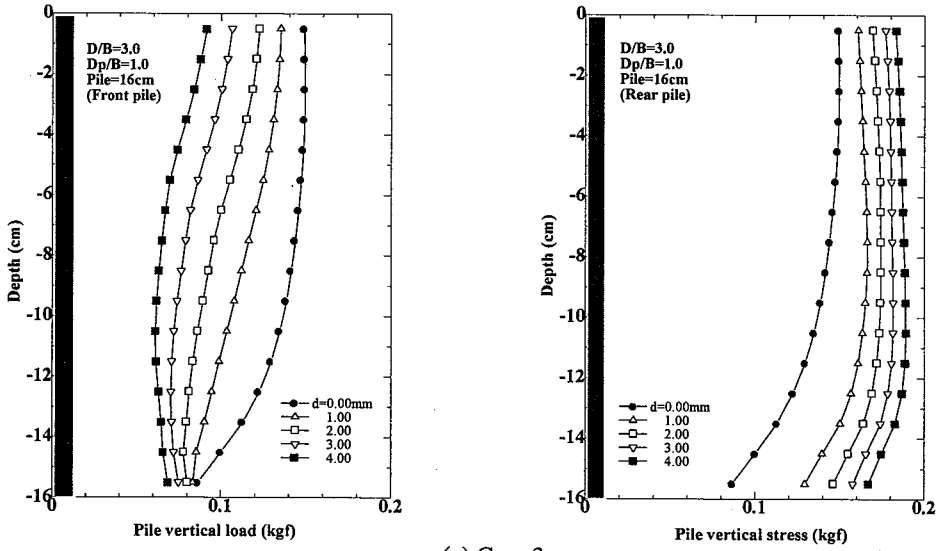

(c) Case 3

Fig. 13: Distribution of the vertical axial load of the pile (front and rear piles)

Figure 15 represents the percentage of the total load for the raft, the front pile and the rear pile at different stage of the tunnel excavation. It is seen in this figure that the load of the raft and the both piles does not change so much in case 2 where D_p/B=2.0. It is because the inclination of the piled raft in case of D_p/B=2.0 is not so much noticeable. In contrast, since the pile tip is closer to the excavation block in case 1 and case 3, the piled raft tilts more and the relative

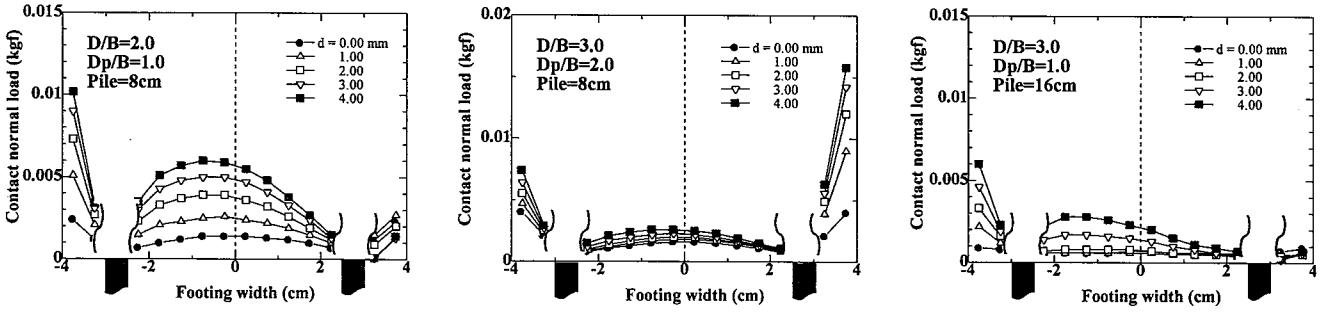

(a) case 1 (b) case 2 (c) case 3

Fig. 14: Distribution of the contact normal load beneath the raft

movements of the pile and the surrounding ground become large, which leads a significant reduction of the axial load of the front pile and an increase vertical load of the raft. In case 3, the increase of the vertical load of the raft is lower than that in case 1. This is because in case 3 the length of the pile is 16cm which is long enough to have large shaft friction.

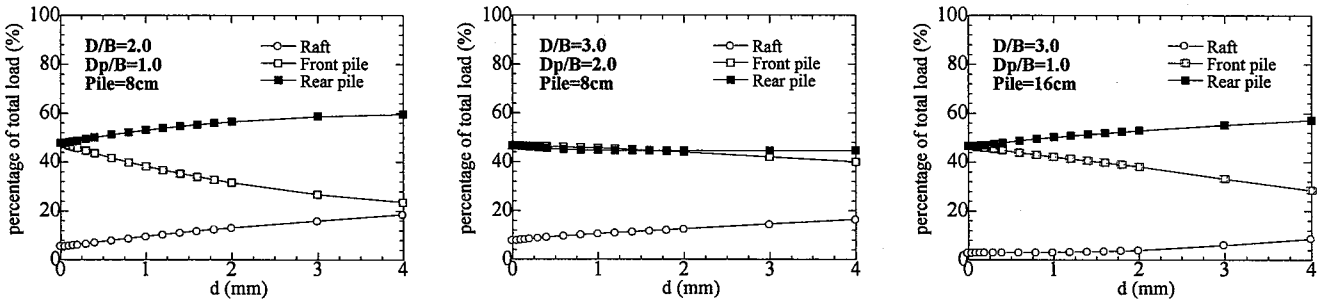

(a) case 1 (b) case 2 (c) case 3

Fig. 15: Percentage of total load in the piled raft

4.3 *Effect of existing load on pile bearing capacity*

When the interaction problem between tunnel and pile foundation is studied, usually existing load like building load is not considered in the analysis of the interaction of tunnel and pile foundation. In this section the effects of the magnitude of the existing load for the piled raft is discussed based on the results of the finite element analyses. Two types of loading levels are considered in these analyses. The amount of the load for loading type 1 is 3.136 N/cm, and Q_v=5.88 N/cm is used for loading type 2. Figure 16 illustrates the rotation of the raft (cap) with the excavation of the tunnel for two types of the initial dead load, where (a) represents the results of the applied load Q_v=3.136 N/cm, and (b) shows the results of the applied load Q_v=5.88 N/cm. In case 2 for the applied load Q_v=3.136 N/cm, the rotation of the raft is not noticeable. However, for the applied load Q_v=5.88 N/cm, a significant rotation of the raft in the clockwise direction (figure 16(b)) is seen in case 2 due to the development of the shear band from the excavation block to the rear pile of the piled raft (Figure 8). Almost the same amount of the rotation is seen in case 1 and case 3 for both loading conditions. It is, therefore, can be said that the rotation of the existing structure is very much dependent on the distance between the pile tip and the crown of the tunnel. For D_p/B greater than 1.0, the influence of the existing load on the rotation of the existing structure is more.

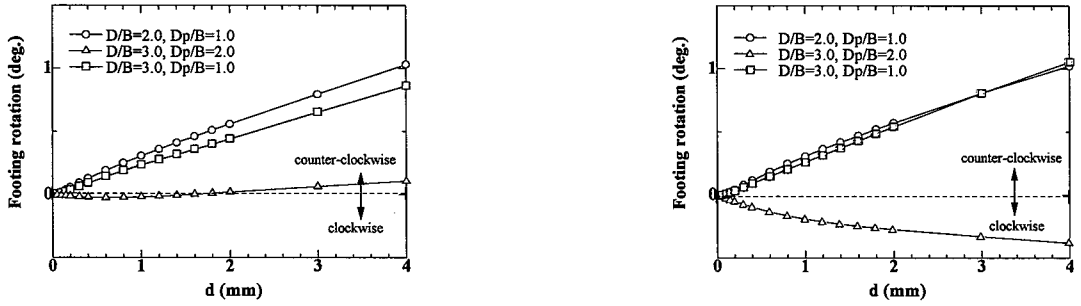

(a) piled raft (Q_v=3.136 N/cm) (b) piled raft (Q_v=5.88 N/cm)

Fig. 16: Rotation angle of the raft (cap) for the piled raft

Figures 17 and 18 represent the results of numerical analyses for the existing load Q_v=3.136 N/cm and Q_v =5.88 N/cm, respectively, where figure (a) represents the distribution of vertical load of the piles, (b) shows the settlements of the pile and the ground around the pile, and figure (c) illustrates the shaft friction load. Here, the vertical load of the pile is calculated from the vertical stress of the element of the pile at every excavation step. The settlement of the pile is the vertical displacement of pile node after completion of the excavation (d=4mm). The shaft friction load of the pile is calculated by the difference of the vertical load of the pile head and the position along the depth of the pile at every excavation step. It is seen in these figures that the occurrence of the settlements is different between these loading conditions. When exiting load is 3.136 N/cm, the ground settlement is larger than the settlement of the front pile, but the settlement of the rear pile is larger than the ground settlement. However, for Q_v =5.88 N/cm the settlement of the both piles are larger than the settlement of the ground. For the larger settlement of the ground around the front pile in case of Q_v=3.136 N/cm, negative friction is developed on the face of the front pile. In contrast, the larger settlement of the pile produces positive friction on the face of the pile. The differential settlement is seen in the piled raft, and it is also varied according to the magnitude of the loading.

The shaft resistance is influenced by the differential settlement. In Figure 17(a), it is seen that the vertical load at the head of the pile decreases more than the tip due to the development of the negative friction. It is also seen in Figure 17(c), the shaft friction load decreases significantly with the excavation step as negative friction is developed at the front pile of the piled raft. However, for the settlement of the pile larger than the ground like figure 18(b) the reduction of the shaft friction is less compare to the negative friction. Higher relative settlement between the pile and the ground results more reduction of the shaft friction. For this reason, the shaft friction at the tip of the pile decreases more than the head of the pile.

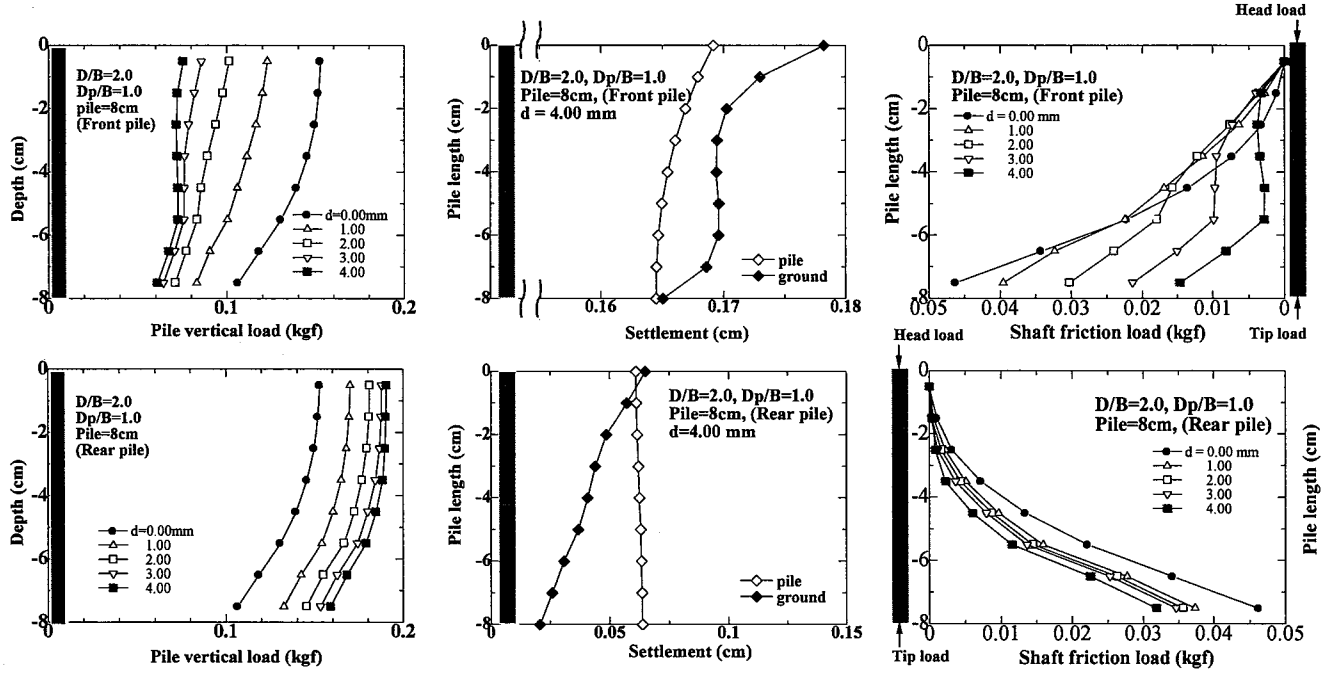

(a) change of pile vertical load (b) settlement of pile and ground (c) change of shaft friction

Fig. 17: Relation of the pile vertical load, shaft friction and relative settlement (3.136 N/cm)

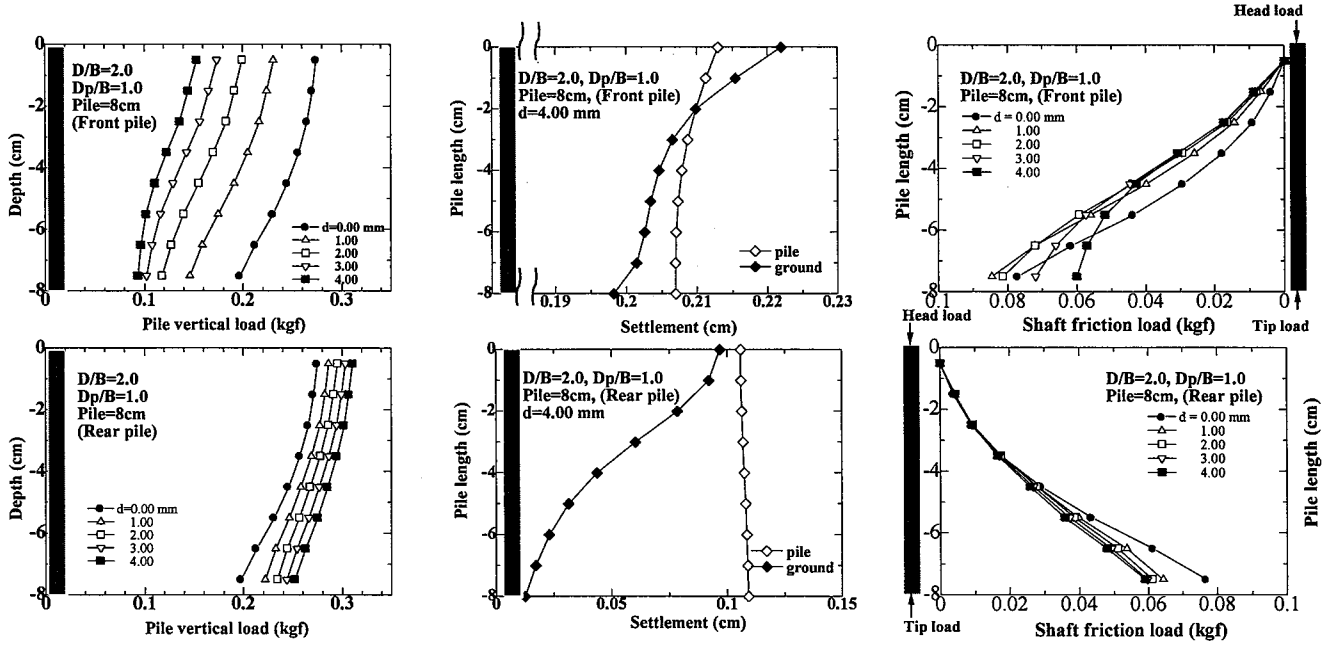

(a) change of pile vertical load (b) settlement of pile and ground (c) change of shaft friction

Fig. 18: Relation of the pile vertical load, shaft friction and relative settlement (5.88 N/cm)

CONCLUSION

To investigate the interaction problems of pile foundation and tunneling, 2D model test and elastoplastic finite element analyses are carried out. The influences of pile type, soil cover, pile length and intensity of existing loading size on the behavior of piled raft are investigated. Although this interaction of the tunneling and the pile foundation is 3D problem to understand the mechanisms and effect factors, all study has been made under 2D condition. From the model tests and numerical analyses, the following points can be concluded:

(1) For the group pile and the piled raft, unsymmetrical earth pressure distribution is observed at the level to the tunnel due to the change of the initial stress of the ground.
(2) The inclination of the group pile or piled raft depends on the distance between the pile tip and the excavation block (D_p). The closer the pile tip from the excavation block, the more inclination of the existing structure towards the excavation place is seen. Therefore, the distance between the pile tip and the crown of the tunnel is more important than the pile length in the interaction problem of tunneling and pile foundation.
(3) The deformation zone of the ground spreads towards the pile from the tunnel crown. Surface settlement troughs for tunnel excavation in case of existing group pile or piled raft are different from green field condition.
(4) The vertical load of the front pile which is nearer to the excavation block decreases significantly with the tunnel excavation. In contrast, the vertical load of the rear pile increases with the excavation of the tunnel.
(5) The relative settlement of soil and pile is an important factor to the development of the shaft friction due to tunneling. Higher relative settlement between the pile and the ground results more reduction of the shaft friction.
(6) Surface settlement and earth pressures of the ground due to tunnel excavation are also dependent on the magnitude of the load of the existing structure.

REFERENCE

1) Jacobsz, S. W., Standing, J. R., Mair, R. J., Hagiwara, T., and Sugitama, T. (2004): Centrifuge modeling of tunnelling near driven piles, *Soils and Foundation*, 44(1), 49-56.
2) Loganathan, N., Poulos, H. g., and Xu, K. J. (2001): Ground and pile-group responses due to tunneling, *Soils and Foundation*, 41(1), 57-67.
3) Nakai, T. (1985): Finite element computations for active and passive earth pressure problems of retaining wall, *Soils and Foundation*, 25(3), 98-112.
4) Nakai, T., Xu, L. & Yamazaki, H. (1997): 3D and 2D model tests and numerical analyses of settlements and earth pressure due to tunnel excavation, *Soils and Foundations*, 37(3), 31-42.
5) Nakai, T., and Hinokio, M. (2004): A simple elastoplastic model for normally and over consolidated soils with unified material parameters, *Soils and Foundation*, 44(2), 53-70.
6) Shahin, H. M., Nakai, T., Hinokio, M., Kurimoto, T., and Sada, T. (2004): Influence of surface loads and construction sequence on ground response due to tunneling, *Soils and Foundation*, 44(2), 71-84.